CrossMark

TRANSLATIONAL RESEARCH

Regional Differences in Cerebral Glucose Metabolism After Cardiac Arrest and Resuscitation in Rats Using [18F]FDG Positron Emission Tomography and Autoradiography

Alessandro Putzu[1,2] · Silvia Valtorta[3,4] · Giuseppe Di Grigoli[3,5] · Matthias Haenggi[6] · Sara Belloli[3,5] · Antonio Malgaroli[7] · Marco Gemma[1,2] · Giovanni Landoni[1,2] · Luigi Beretta[1,2] · Rosa Maria Moresco[3,4]

Abstract

Background Cardiac arrest is an important cause of morbidity and mortality. Brain injury severity and prognosis of cardiac arrest patients are related to the cerebral areas affected. To this aim, we evaluated the variability and the distribution of brain glucose metabolism after cardiac arrest and resuscitation in an adult rat model.

Methods Ten rats underwent 8-min cardiac arrest, induced with a mixture of potassium and esmolol, and resuscitation, performed with chest compressions and epinephrine. Eight sham animals received anesthesia and experimental procedures identical to the ischemic group except cardiac arrest induction. Brain metabolism was assessed using [18F]FDG autoradiography and small animal-dedicated positron emission tomography.

Results The absolute glucose metabolism measured with [18F]FDG autoradiography 2 h after cardiac arrest and resuscitation was lower in the frontal, parietal, occipital, and temporal cortices of cardiac arrest animals, showing, respectively, a 36% ($p = 0.006$), 32% ($p = 0.016$), 36% ($p = 0.009$), and 32% ($p = 0.013$) decrease compared to sham group. Striatum, hippocampus, thalamus, brainstem, and cerebellum showed no significant changes. Relative regional metabolism indicated a redistribution of metabolism from cortical area to brainstem and cerebellum.

✉ Rosa Maria Moresco
moresco.rosamaria@hsr.it

Alessandro Putzu
alessandroputzu@ymail.com

Silvia Valtorta
valtorta.silvia@hsr.it

Giuseppe Di Grigoli
digrigolig@gmail.com

Matthias Haenggi
matthias.haenggi@insel.ch

Sara Belloli
belloli.sara@hsr.it

Antonio Malgaroli
malgaroli.antonio@unisr.it

Marco Gemma
gemma.marco@hsr.it

Giovanni Landoni
landoni.giovanni@hsr.it

Luigi Beretta
beretta.luigi@hsr.it

[1] Department of Anesthesia and Intensive Care, IRCCS San Raffaele Scientific Institute, Milan, Italy

[2] Vita-Salute San Raffaele University, Milan, Italy

[3] Experimental Imaging Center, IRCCS San Raffaele Scientific Institute, Milan, Italy

[4] Department of Medicine and Surgery, University of Milano-Bicocca, Via Cadore 48, 20900 Monza, MB, Italy

[5] IBFM-CNR, Milan, Italy

[6] Department of Intensive Care Medicine, Inselspital, Bern University Hospital, University of Bern, Bern, Switzerland

[7] Neurobiology of Learning Unit, Division of Neuroscience, Vita-Salute San Raffaele University, Milan, Italy

Conclusions Our data suggest that cerebral regions have different susceptibility to moderate global ischemia in terms of glucose metabolism. The neocortex showed a higher sensibility to hypoxia–ischemia than other regions. Other subcortical regions, in particular brainstem and cerebellum, showed no significant change compared to non-ischemic rats.

Introduction

Cardiac arrest is a leading cause of death among adults worldwide. In the USA alone, approximately 580,000 patients suffer sudden cardiac arrest every year, with an average overall survival rate at hospital discharge of 9.5% [1, 2]. Recent studies suggest that 6 months after the ischemic insult up to 70% of survivors have a good cerebral performance and a functional independence [3, 4]. However, neuropsychological deficits are common, including memory, executive, and perceptive deficits in up to two-third of cardiac arrest survivors [4–6]. All these findings suggested some degree of cortical dysfunction after cardiac arrest and resuscitation.

The physiopathological events during and after brain ischemia are very complex and partially a matter of conjecture. The mammalian brain depends mainly on glucose as source of energy [7, 8], thus requiring a tight regulation of glucose supply. In addition, the complex neurons–glia interaction for energy maintenance, synaptic activity and neurons protections clearly support a main role of glucose metabolism in brain functions, plasticity, and neuron survival [9, 10].

Positron emission tomography (PET) and autoradiography permit to evaluate brain metabolism thanks to the administration of [18F]fluorodeoxyglucose (FDG), a glucose analogue lacking of 2-hydroxyl group, which is taken up by cerebral cells according to energy demands, where it is retained after phosphorylation by hexokinases [11].

The effect of cardiac arrest on regional glucose metabolic pattern was described in a limited number of clinical and preclinical PET studies [12–19]. Common conclusions of these studies are that cardiac arrest produces a marked depression of glucose metabolism that persists for several hours [13–15, 20]. However, most of published studies did not aim to the evaluation of the regional vulnerability of brain tissue to the hypoxic-ischemic insult caused by cardiac arrest. Since the prognosis of cardiac arrest in patients is tightly related to the degree of ischemic injury and to its regional distribution, we employed a rat model of asystolic cardiac arrest to explore early regional modifications in brain glucose metabolism after cardiac arrest and resuscitation using the glucose analogue [18F]FDG.

Methods

Subjects

Experiments were approved by the Italian and Local Ethics Committees for Institutional Animal Care and Use (no. 206/2015-PR) and carried out in accordance with the Italian and European recommendations for the care and use of laboratory animals. Male CD rats (Charles River Laboratories, Italy) weighting 340 g were housed in a temperature-controlled environment (22 °C) under a 12:12 h dark/light cycle and free access to food and water. All animals were fasted with free access to water from the night before the experiments.

Experimental Protocol

Animals were allocated into two groups: ten rats underwent 8-min cardiac arrest (cardiac arrest group), whereas eight rats were used as controls (sham group). Sham animals were treated similarly to cardiac arrest group, except cardiac standstill and cardiopulmonary resuscitation procedures.

The study protocol consisted of surgical preparation, induction of cardiac arrest and resuscitation, stabilization, PET imaging, euthanasia, and autoradiography (Fig. 1). The anesthesia was induced with desflurane 14% (Suprane, Baxter, Italy) in an anesthesia chamber until unconsciousness. Topical spray lidocaine 4% (SALF Laboratorio Farmacologico, Italy) was sprayed in the oropharyngeal cavity, and tracheal intubation was performed using a 16-gauge catheter. Animals were mechanically ventilated with a ventilator (Servo 900, Siemens AG, Germany), in volume control mode and 21% oxygen. Ventilation was adapted after the first blood gas analysis (BGA). The right femoral artery was catheterized using polyethylene tubing (PE 50 mm I.D.) for blood sampling and continuous monitoring of mean arterial blood pressure (MAP). The right jugular vein was catheterized (PE 50 mm I.D.) for intravenous drugs administration and fluid infusion. Two electrocardiography (ECG) electrodes were subcutaneously placed on the chest. Rectal temperature was monitored and maintained between 36.5 and 37.5 °C using a heating lamp throughout the whole experiment. All the surgical procedures were carried out under desflurane 7% anesthesia and subcutaneous lidocaine 4%. After surgical procedures, anesthesia was maintained with desflurane 5%.

In order to assess the impact of experimental conditions (e.g., surgery, anesthesia) on regional brain metabolism,

Fig. 1 Timeline of experimental procedure. *CA* cardiac arrest, *CPR* cardiopulmonary resuscitation, *PET* positron emission tomography, *min* minutes, *FDG* [18F]fluorodeoxyglucose
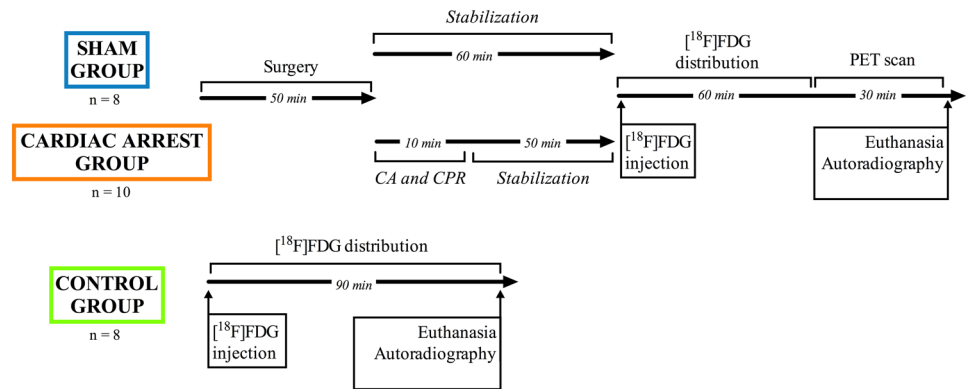
eight additional animals (control group) were studied without any surgical procedures and any anesthesia, except before euthanasia, and compared with sham group. In this last group regional brain metabolism was evaluated using only postmortem autoradiography (see below).

Recordings and Measurements

Rectal temperature, MAP, heart rate, and single channel ECG were displayed and registered continuously on a monitor (Agilent M1205A, Agilent Technologies, USA). Arterial acid–base measurements were performed on blood obtained from the femoral artery catheter and immediately analyzed immediately on a blood gas analyzer (Opti CCA, Opti Medical System, USA). Plasma glucose was estimated using a glucometer (StatStrip Xpress-i, Nova Biomedical, USA).

Cardiac Arrest and Resuscitation

At the end of surgical procedures, anaesthetized rats were paralyzed with vecuronium 2 mg/kg (Norcuron, Organon Teknika BV, Netherlands). Five minutes after injection, cardiac arrest was induced with a mixture of potassium chloride (Braun, Germany) and esmolol (Brevibloc, Baxter Healthcare, UK), using the procedure described by Bendel et al. [21] previously set up and validated on Wistar rats. In this study, CD rats were selected in order to test the experimental procedure on another rat strain and to use our [18F]FDG brain template for PET images analysis. Cardiac arrest was defined as a MAP below 15 mmHg. Just after the induction of cardiac arrest, inhalation anesthesia and ventilation were stopped, and the heating lamp turned off. Eight minutes after induction of cardiac arrest, cardiopulmonary resuscitation (CPR) was initiated with manual metronome-guided external chest compression with two fingers at a rate of 220 bpm, ventilation resumed with fraction of inspired oxygen (FiO2) of 100%, and the heating lamp turned on. Uninterrupted chest compressions were

always made by the same operator, with quality assessed by MAP waveform analysis. A single dose of diluted epinephrine (15 µg/kg) (SALF Laboratorio Farmacologico, Italy), followed by a single dose of calcium gluconate (15 µg/kg) (SALF Laboratorio Farmacologico, Italy), was injected intravenously. Restoration of spontaneous circulation (ROSC) was defined as spontaneous MAP over 65 mmHg, sustained for at least 30 s. If ROSC was not achieved within 60 s, epinephrine was repeated with 5 µg/kg every 30 s until ROSC. ROSC had to be achieved within 180 s; otherwise, the experiment was out of protocol and animals were excluded. Controlled ventilation was continued after cardiac arrest until the end of the experiment. In the 25 min after ROSC, FiO2 was progressively decreased to 21% and desflurane concentration gradually increased up to 5%. BGA was performed 22 min after ROSC and, accordingly, ventilator settings adapted. Just after blood analysis, catheters were withdrawn and wounds closed.

Positron Emission Tomography Study

At the end of stabilization period (50 min), cardiac arrest and sham groups' animals were transferred to the PET bed, placed in a prone position on a movable tabletop, with the fixed head centered in the scanner. [18F]FDG was prepared for clinical use (European Pharmacopeia VIII Edition) and injected intravenously in tail vein (35.37 ± 2.92 MBq in 0.2 ml of normal saline). One hour after the injection, brain radioactivity concentration was acquired for 30 min (6 frames of 5 min each) under desflurane 5% anesthesia. PET images were then reconstructed with the expectation maximization algorithm, calibrated with a calibration phantom to transform count per voxel values in MBq/g and corrected for 18F half-life (109.8 min.). Our [18F]FDG PET images were co-registered to [18F]FDG PET Rat template of PMOD (PMOD 2.7, PMOD Technologies, Switzerland) software [22]. After that, on co-registered images we applied Rat Brain volume of interest (VOI) template atlas

to obtain radioactivity values [23]. [18F]FDG uptake in each area was expressed as mean standardized uptake value (SUV mean) using the following formula: (mean radioactivity measured in the VOI/injected radioactivity)*animal weight.

Autoradiography Study

At the end of PET study, desflurane concentration was turned to 18% and cardiac arrest and sham animals were decapitated and brain processed for autoradiography. As previously indicated, control group animals were processed for autoradiography as described above at 90 min after [18F]FDG injection. For all groups, brains were rapidly removed, placed in Brain Matrix (Stoelting Co, USA) and cut into coronal slices (2 mm) that were exposed to phosphor screen (Perkin Elmer, USA) for 1 h in a dark room and developed with a Cyclone Storage Phosphor System (Perkin Elmer, USA). To determine brain radioactivity concentration, region of interests were defined using OptiQuant software (Perkin Elmer, USA) and rat brain atlas [23]. Optical concentration units expressed as digital light units/mm^2 were transformed into radioactivity concentration units (MBq/mm^2) using a standard calibration curve and corrected for injected dose and then expressed as percentage of injected dose per mm^2 (%ID/mm^2), representing the 'absolute glucose metabolism.' Data are presented also as 'relative glucose metabolism,' where regional absolute [18F]FDG uptake values were divided for the mean values of [18F]FDG uptake in the whole brain. This second type of analysis, used also in clinical research with [18F]FDG PET, reduces the high variability of brain metabolism values present also at rest, showing the regional metabolic reorganization of brain metabolism induced by a certain condition.

Statistical Analysis

Data were analyzed using GraphPad Prism version 6 (GraphPad Software, La Jolla, CA, USA). Significance of the differences between groups was analyzed by unpaired two-tailed Student's t test or one-way ANOVA followed by Bonferroni post hoc test as appropriate. Significance was indicated by $p < 0.05$. Results are expressed as mean value ± standard deviation and percentage variation (%). Sample size calculation was performed according to the results of a previous study on brain metabolism [24]: eight animals per group were necessary to demonstrate a decrease in cortical metabolism of 40% with a power of 90% at 5% level with a standard deviation of 25%; since we expected an unsuccessful resuscitation rate of about 25% in the cardiac arrest group, we added two animals to this group.

Results

Cardiac Arrest and Resuscitation

The two interventional groups, cardiac arrest and sham, did not differ in term of baseline and experimental variables (eTable 1, Supplementary Material). After cardiac arrest induction, the MAP of the cardiac arrest group immediately fell to 5.18 ± 2.49 mmHg and stabilized after resuscitation maneuvers (eFigure 1, Supplementary Material). Temperature was stable in both groups (eFigure 2, Supplementary Material). There were no statistical significant differences in the acid–base values prior to cardiac arrest (eTable 2, Supplementary Material). Blood gas analysis of the cardiac arrest rats showed a significant increase in PaO$_2$ from 14.71 ± 1.83 to 22.40 ± 4.89 kPa ($p < 0.01$), due to the higher FiO$_2$ during CPR, associated with a significant decrease in base excess (2.45 ± 1.72 vs. −5.07 ± 2.26 mmol/L, $p < 0.01$) and bicarbonate (23.45 ± 3.77 vs. 17.19 ± 3.18 mmol/L, $p < 0.01$), owing to the metabolic acidosis that occurs during cardiac arrest.

Cardiac arrest was induced in all animals of cardiac arrest group, and CPR was successful in nine of these ten animals with ROSC achieved 98 ± 41 s after CPR initiation. Cumulative epinephrine administration was 25 ± 7 μg/kg.

Cardiac Arrest Impaired Glucose Metabolism Particularly in Cortical Regions

By examining absolute uptake values obtained in autoradiographic images analysis, the study revealed that anesthesia per se reduced global glucose metabolism both in sham and cardiac arrest group in comparison with control
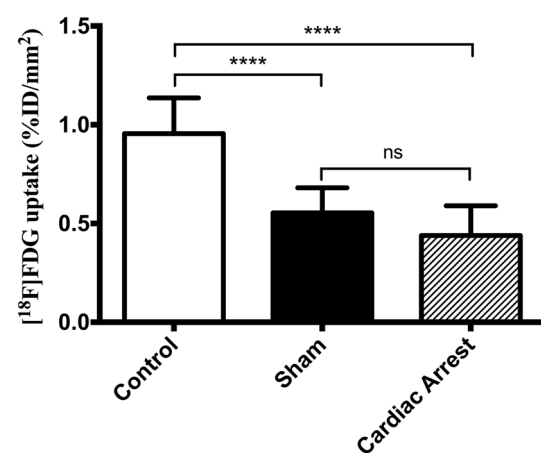
Fig. 2 Global cerebral metabolism measured using autoradiography imaging: absolute [18F]FDG uptake (%ID/mm^2) in cardiac arrest, sham, and control groups. Data shown as mean ± SD. *FDG* [18F]fluorodeoxyglucose, *SD* standard deviation. ****p value <0.0001
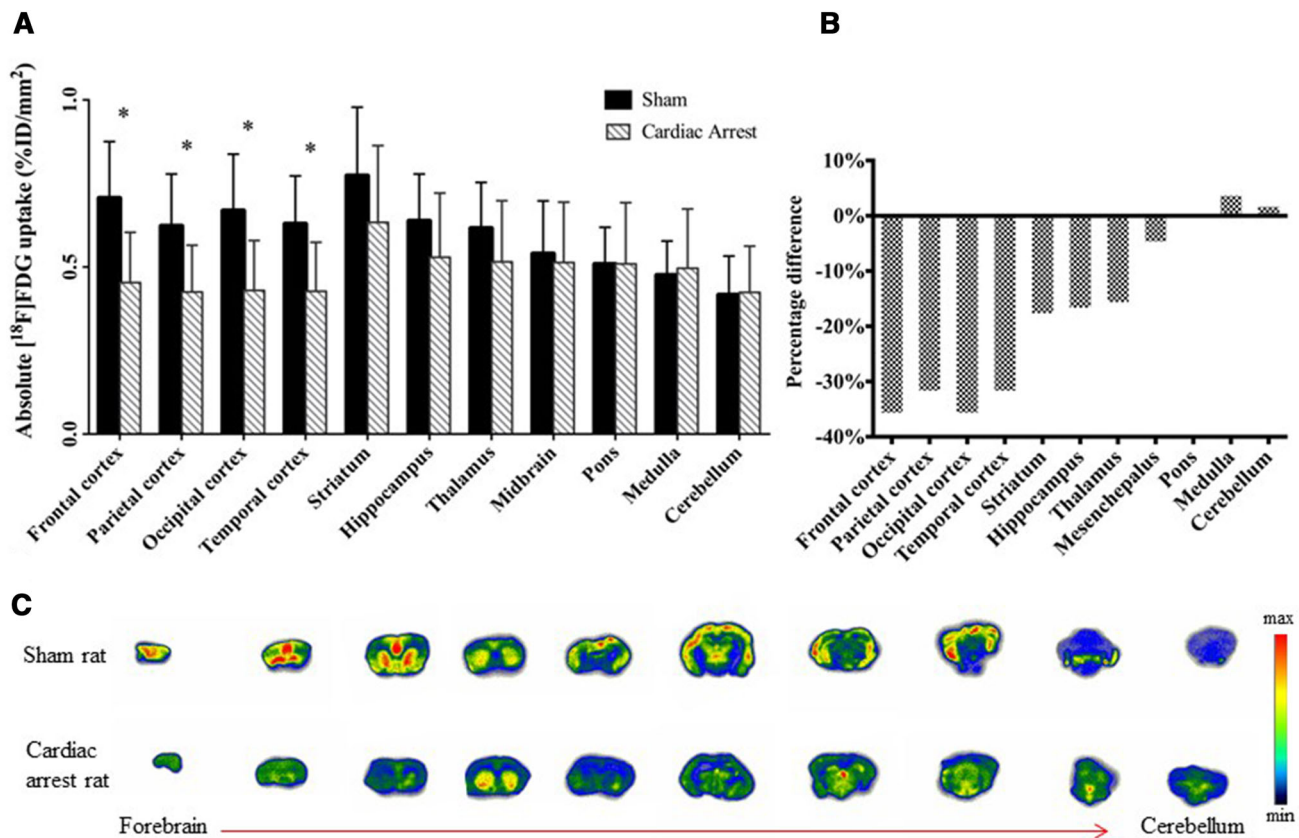
Fig. 3 Regional cerebral metabolism measured using autoradiography imaging. **a** Absolute [^{18}F]FDG uptake (%ID/mm^2) in cardiac arrest and sham groups in different cerebral areas. Data shown as mean ± SD. *p value < 0.05. **b** Percentage variation of absolute

[^{18}F]FDG uptake (%ID/mm^2) in cardiac arrest and sham groups. Data shown as mean (%). **c** Representative cerebral slices at autoradiography study of a sham and a cardiac arrest animal. *FDG* [^{18}F]fluorodeoxyglucose, *SD* standard deviation

condition ($p < 0.0001$) (Fig. 2; eTable 3, Supplementary Material).

Cardiac arrest reduced absolute [^{18}F]FDG uptake from −32 to −36% in all cortical areas compared to sham animals (Fig. 3a; eTable 4, Supplementary Material). Although a trend over a reduction was observed in the striatum, hippocampus, and thalamus (−18, −17, and −16%, respectively), the effect was not statistically significant. No modifications were observed in posterior brain regions like cerebellum and brainstem (−5 to +4%) (Fig. 3b). A typical example of variation of cerebral glucose metabolism is given in autoradiographic images of Fig. 3c.

When assessing the relative regional metabolism, we evidenced a significant reduction in relative [^{18}F]FDG uptake in the cortical areas, with an increase up to 33% in posterior regions like midbrain, pons, and cerebellum (Fig. 4; eTable 5, Supplementary Material), indicating a redistribution of energy utilization caused by the lower metabolic vulnerability of these last regions to the ischemic insult.

Similarly, in PET images we observed a trend of decrement of absolute metabolism in cortical areas ($p = 0.04$ for frontal cortex) of cardiac arrest group and a similar metabolic pattern in brainstem and cerebellum (eFigure 3, Supplementary Material).

When studying the effects of experimental confounding factors (e.g., anesthesia, surgery) on regional brain metabolism comparing sham and control unanesthetized rats, we found that these factors decreased regional brain metabolism in a uniform manner of approximately 45% (eTable 6, Supplementary Material).

Discussion

At preclinical level, effects of cardiac arrest and resuscitation on regional cerebral metabolic pattern have not been extensively investigated. This is the first study designed with this aim. We found a significant decrease in neocortical metabolism (32–36%) in post-ischemic rats, thus confirming the high vulnerability of the cortex to ischemic
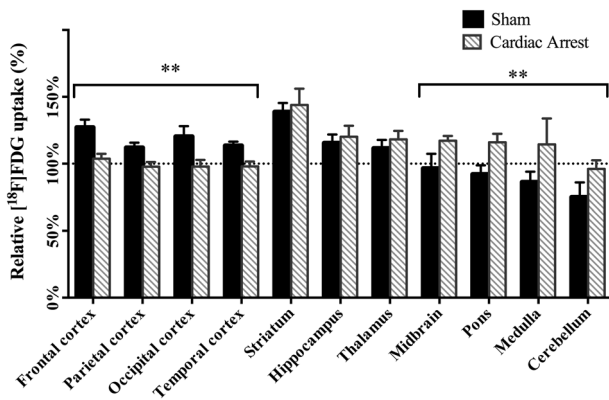
Fig. 4 Regional cerebral metabolism measured using autoradiography imaging: relative [18F]FDG uptake (%) in cardiac arrest and sham groups. Regional [18F]FDG uptake was normalized to whole brain metabolism. Data shown as mean ± SD. *FDG* [18F]fluorodeoxyglucose, *SD* standard deviation. **p value <0.01

insult [12, 13, 16]. On the contrary, deep structures, such as brainstem and cerebellum, which are also phylogenetically the oldest, were not affected by cardiac arrest. Interestingly, relative metabolism data suggest that, after global ischemia, brain metabolism underwent major modifications and redistribution in favor of midbrain, pons, and cerebellum, to the detriment of neocortical regions. Our results are in line with clinical findings on cardiac arrest patients where a mild-to-moderate hypoxic-ischemic encephalopathy is usually present as early severe cortical dysfunction, with a relative preservation of brainstem function. No [18F]FDG PET data are available from cardiac arrest human survivors presenting mild-to-moderate encephalopathy; however, data from patients with higher degree of encephalopathy indicate a greater reduction in cortical brain metabolism when compared with subcortical or deep regions [16, 19].

Cortical neurons are known to be very sensible to ischemia [25–28]. De Lange et al. evaluated metabolism with [18F]FDG PET in a piglet perinatal hypoxia cardiac arrest model. In partial agreement with our findings, they showed a marked reduction in metabolism at approximately 3 h after resuscitation that was maximum in the cortex but involved also the basal ganglia and cerebellum [15]. Ischemic damage to specific brain structures, due to immediate or delayed cellular death, mainly includes pyramidal neurons of the CA1 area of the hippocampus, neurons in layers 3 and 5 of the cerebral cortex, Purkinje cells of the cerebellum, and spiny neurons in the striatum [18, 27, 28].

Hippocampal neurons are widely studied in experimental models of cardiac arrest. Five to ten minutes of global cerebral ischemia determine a delayed apoptotic neuronal death of pyramidal CA1 neurons in hippocampus that culminates at 2–3 days after injury [29, 30]. A time-dependent increasing damage of hippocampal neurons has

been described postmortem also in patients [31] and the clinical follow-up of survivors suggested an impairment of this region [32]. In our study, we failed to find significant decrease in glucose metabolism in this area. A lack of hippocampal impairment is in agreement to what reported by Blomqvist and Wieloch [14], indicating a lack of an early large metabolic impairment after injury, even if a relatively small decrease could not be excluded. Subcortical brain structures, like thalamus, hypothalamus, and brainstem, are less sensitive to ischemic injury [27, 33, 34]. Indeed, our findings indicated a lesser degree of absolute metabolic impairment in these regions and a redistribution of relative glucose metabolism, suggesting that after mild-to-moderate ischemia the rate of glucose consumption is preserved in cerebellum and brainstem, whereas metabolism is impaired in neocortical areas. Follow-up studies in cardiac arrest survivors showed that alterations in arousal and consciousness, functions directed by the brainstem, are not predominant, since consciousness with different grade of cognitive dysfunction is rather common [35]. On the other hand, a general depression of regional brain function and metabolism was demonstrated only after severe ischemia, with a trend over a greater reduction in cortical areas [16]. Interestingly, a consciousness-level-dependent preservation of regional brain metabolism was observed in cortical and subcortical areas but not in other regions like cerebellum or brainstem [36].

Several experimental parameters could be source of possible alteration of relevant experimental endpoints, such as brain metabolism [37]. To avoid potential confounding effects on brain metabolism induced by anesthesia, acute stress conditions secondary to surgery or mechanical ventilation, and modification in body temperature [38], the cardiac arrest group was compared with a sham operated group of rats receiving anesthesia and all experimental procedures but no cardiac arrest. It is well known that halogenated anesthetics (e.g., desflurane) affect brain metabolism [39, 40]. To further test the effect of desflurane, we added a control group of freely moving animals anesthetized only for euthanasia. In agreement with other studies, we observed that anesthesia induced a uniform decrease in [18F]FDG retention all over the brain [39].

Strengths and Limitations

The validity of this cardiac arrest model was well documented [21, 41, 42]. In our setting it showed low variability, confirming the good quality and high reproducibility of the model both in Wistar rats, as previously observed [21], and also in CD rats, as described here. The ischemic insult was of predetermined duration, with low variability in cardiac arrest onset and ROSC. Furthermore, ischemia strikes the whole nervous system and the whole

organism, leading to a post-resuscitation syndrome, on the contrary of some global brain ischemia models (e.g., 4-vessels occlusion models) [12, 13]. Our model showed no post-ischemic complications, and the overall survival rate was 90%, showing that this model is clinically relevant for the study of a mild-to-moderate hypoxic-ischemic encephalopathy [21, 41, 42]. Vasoactive medicaments (e.g., epinephrine) were not administered to animals after resuscitation, since these drugs could alter brain physiology and their use could be linked to a worse outcome after cardiac arrest [43]. As previously stated, to keep under control possible confounders of the procedure (e.g., anesthesia, surgery), a sham group was added.

In our study we observed a decrease in neocortex and no changes of [^{18}F]FDG uptake in cerebellum and brainstem with a consequent redistribution in regional brain metabolism. We failed to find significant differences in subcortical regions like hippocampus, striatum, and thalamus, even if a slight but not significant reduction was detected. Our explorative study was designed and powered to evidence major metabolic differences in cortical regions, for an understanding of pathophysiological processes that follow cardiac arrest. However, the small sample size could partially mask the detection of slight modifications particularly in a small brain region like the hippocampus. It should be noted that positron emitter signal is affected by physical artifacts like partial volume effects or spill over [44] that reduce the capability of the method in the detection of slight metabolic modifications particularly in small brain regions surrounded by high metabolic tissue, like the hippocampus. A specific effect of cardiac arrest on these regions could be tested in further studies designed for this specific objective. For metabolic analysis we applied a simple protocol based on the calculation of absolute or relative value of radioactivity concentration and not a fully quantification model. Despite the potential limits, the semiquantitative approach used in our study is similar to the one used in clinical PET studies and avoids the withdrawal of large amount of blood that could compromised post-cardiac arrest animals.

Future Directions

Cerebral metabolic patterns vary among different post-ischemic neurological conditions, but reduced glucose metabolism remains the hallmark of early and late post-cardiac arrest brain injury in adult humans [16–19, 45]. However, a clear correlation between cerebral glucose metabolism and clinical outcome has not yet been established mainly due to the lack of large clinical trials with survivors presenting different degree of brain injury, with adequate sample size, and standardization of methods and imaging times. In vegetative state and comatose patients,

delayed modifications in glucose metabolism are often indicative of irreversible cerebral damage [45]. On the other hand, postanoxic conscious patients with a moderate degree of cerebral injury could present a marked reduction in cerebral glucose metabolism [16, 17, 19]. Decreasing the degree of early neocortical metabolic injury could be an interesting target, since the consequences of neocortical injury are prominent in cardiac arrest survivors [4–6]. Understanding the early modifications in glucose metabolism after cardiac arrest and how they are related with the clinical outcome is crucial to develop a functional noninvasive endpoint for the early preclinical assessment of the efficacy of novel interventions strategy that can be translated to clinical studies [46, 47]. Finally, using this cardiac arrest animal model, future studies should evaluate the origin and possible modulation of the redistribution of post-ischemic cerebral metabolism, in particular the juxtaposition between neocortical and brainstem/cerebellar metabolism, to evidence if the uncoupling of perfusion to metabolic demand [48] or a reduced metabolism itself is crucial in this condition.

Conclusions

Cardiac arrest and resuscitation induced a significant post-ischemic regional variation of glucose metabolism, as compared to sham non-ischemic rats. After resuscitation, glucose metabolism decreased in frontal, temporal, parietal, and occipital cortex, but did not change significantly in hippocampus, striatum, thalamus, brainstem, and cerebellum, suggesting a selective sensibility of neocortical areas to ischemic insult. Further preclinical studies are warranted to evaluate if modulation of cortical glucose metabolism could be a therapeutic strategy after cardiac arrest.

References

1. Go AS, Mozaffarian D, Roger VL, Benjamin EJ, Berry JD, Borden WB, et al. Heart disease and stroke statistics—2013 update: a report from the American Heart Association. Circulation. 2013;127:e6–245.

2. Chugh SS, Jui J, Gunson K, Stecker EC, John BT, Thompson B, et al. Current burden of sudden cardiac death: multiple source surveillance versus retrospective death certificate-based review in a large US community. J Am Coll Cardiol. 2004;44:1268–75.

3. Graves JR, Herlitz J, Bång A, Axelsson A, Ekström L, Holmberg M, et al. Survivors of out of hospital cardiac arrest: their prognosis, longevity and functional status. Resuscitation. 1997;35: 117–21.

4. Bro-Jeppesen J, Kjaergaard J, Horsted TI, Wanscher MC, Nielsen SL, Rasmussen LS, et al. The impact of therapeutic hypothermia on neurological function and quality of life after cardiac arrest. Resuscitation. 2009;80:171–6.

5. Tiainen M, Poutiainen E, Kovala T, Takkunen O, Häppölä O, Roine RO. Cognitive and neurophysiological outcome of cardiac arrest survivors treated with therapeutic hypothermia. Stroke. 2007;38:2303–8.

6. Torgersen J, Strand K, Bjelland TW, Klepstad P, Kvåle R, Søreide E, et al. Cognitive dysfunction and health-related quality of life after a cardiac arrest and therapeutic hypothermia. Acta Anaesthesiol Scand. 2010;54:721–8.

7. Mergenthaler P, Lindauer U, Dienel GA, Meisel A. Sugar for the brain: the role of glucose in physiological and pathological brain function. Trends Neurosci. 2013;36:587–97.

8. Howarth C, Gleeson P, Attwell D. Updated energy budgets for neural computation in the neocortex and cerebellum. J Cereb Blood Flow Metab. 2012;32:1222–32.

9. Magistretti PJ, Allaman I, Aiello LC, Wheeler P, Allaman I, Magistretti PJ, et al. A cellular perspective on brain energy metabolism and functional imaging. Neuron. 2015;86:883–901.

10. Gao C, Zhou L, Zhu W, Wang H, Wang R, He Y, et al. Monocarboxylate transporter-dependent mechanism confers resistance to oxygen- and glucose-deprivation injury in astrocyte-neuron cocultures. Neurosci Lett. 2015;594:99–104.

11. Reivich M, Kuhl D, Wolf A, Greenberg J, Phelps M, Ido T, et al. The [^{18}F]fluorodeoxyglucose method for the measurement of local cerebral glucose utilization in man. Circ Res. 1979;44: 127–37.

12. Choki J, Greenberg J, Reivich M. Regional cerebral glucose metabolism during and after bilateral cerebral ischemia in the gerbil. Stroke. 1983;14:568–74.

13. Mies G, Paschen W, Hossmann KA. Cerebral blood flow, glucose utilization, regional glucose, and ATP content during the maturation period of delayed ischemic injury in gerbil brain. J Cereb Blood Flow Metab. 1990;10:638–45.

14. Blomqvist P, Wieloch T. Ischemic brain damage in rats following cardiac arrest using a long-term recovery model. J Cereb Blood Flow Metab. 1985;5:420–31.

15. de Lange C, Malinen E, Qu H, Johnsrud K, Skretting A, Saugstad OD, et al. Dynamic FDG PET for assessing early effects of cerebral hypoxia and resuscitation in new-born pigs. Eur J Nucl Med Mol Imaging. 2012;39:792–9.

16. Schaafsma A, de Jong BM, Bams JL, Haaxma-Reiche H, Pruim J, Zijlstra JG. Cerebral perfusion and metabolism in resuscitated patients with severe post-hypoxic encephalopathy. J Neurol Sci. 2003;210:23–30.

17. DeVolder AG, Goffinet AM, Bol A, Michel C, de Barsy T, Laterre C. Brain glucose metabolism in postanoxic syndrome. Positron emission tomographic study. Arch Neurol. 1990;47:197–204.

18. Heiss W-D. PET in coma and in vegetative state. Eur J Neurol. 2012;19:207–11.

19. Rudolf J, Ghaemi M, Ghaemi M, Haupt WF, Szelies B, Heiss WD. Cerebral glucose metabolism in acute and persistent vegetative state. J Neurosurg Anesthesiol. 1999;11:17–24.

20. Li Y-Q, Liao X-X, Lu J-H, Liu R, Hu C-L, Dai G, et al. Assessing the early changes of cerebral glucose metabolism via dynamic (18)FDG-PET/CT during cardiac arrest. Metab Brain Dis. 2015;30:969–77.

21. Bendel S, Springe D, Pereira A, Grandgirard D, Leib SL, Putzu A, et al. Do different anesthesia regimes affect hippocampal apoptosis and neurologic deficits in a rodent cardiac arrest model? BMC Anesthesiol. 2015;15:2.

22. Schiffer WK, Mirrione MM, Biegon A, Alexoff DL, Patel V, Dewey SL. Serial microPET measures of the metabolic reaction to a microdialysis probe implant. J Neurosci Methods. 2006;155: 272–84.

23. Paxinos G, Watson C. The rat brain in stereotaxic coordinates. Amsterdam: Elsevier; 2007.

24. Kozuka M, Smith ML, Siesjö BK. Preischemic hyperglycemia enhances postischemic depression of cerebral metabolic rate. J Cereb Blood Flow Metab. 1989;9:478–90.

25. Sieber FE, Palmon SC, Traystman RJ, Martin LJ. Global incomplete cerebral ischemia produces predominantly cortical neuronal injury. Stroke. 1995;26:2091–5.

26. Welsh JP, Yuen G, Placantonakis DG, Vu TQ, Haiss F, O'Hearn E, et al. Why do Purkinje cells die so easily after global brain ischemia? Aldolase C, EAAT4, and the cerebellar contribution to posthypoxic myoclonus. Adv Neurol. 2002;89:331–59.

27. Brisson CD, Hsieh Y-T, Kim D, Jin AY, Andrew RD. Brainstem neurons survive the identical ischemic stress that kills higher neurons: insight to the persistent vegetative state. PLoS ONE. 2014;9:e96585.

28. Centonze D, Marfia GA, Pisani A, Picconi B, Giacomini P, Bernardi G, et al. Ionic mechanisms underlying differential vulnerability to ischemia in striatal neurons. Prog Neurobiol. 2001;63:687–96.

29. Kirino T. Delayed neuronal death in the gerbil hippocampus following ischemia. Brain Res. 1982;239:57–69.

30. DeLeo J, Toth L, Schubert P, Rudolphi K, Kreutzberg GW. Ischemia-induced neuronal cell death, calcium accumulation, and glial response in the hippocampus of the Mongolian gerbil and protection by propentofylline (HWA 285). J Cereb Blood Flow Metab. 1987;7:745–51.

31. Petito CK, Feldmann E, Pulsinelli WA, Plum F. Delayed hippocampal damage in humans following cardiorespiratory arrest. Neurology. 1987;37:1281–6.

32. Sulzgruber P, Kliegel A, Wandaller C, Uray T, Losert H, Laggner AN, et al. Survivors of cardiac arrest with good neurological outcome show considerable impairments of memory functioning. Resuscitation. 2015;88:120–5.

33. Fujioka M, Okuchi K, Sakaki T, Hiramatsu K, Miyamoto S, Iwasaki S. Specific changes in human brain following reperfusion after cardiac arrest. Stroke. 1994;25:2091–5.

34. Wijdicks EF. The diagnosis of brain death. N Engl J Med. 2001;344:1215–21.

35. Fugate JE, Moore SA, Knopman DS, Claassen DO, Wijdicks EFM, White RD, et al. Cognitive outcomes of patients undergoing therapeutic hypothermia after cardiac arrest. Neurology. 2013;81:40–5.

36. Di Perri C, Bahri MA, Amico E, Thibaut A, Heine L, Antonopoulos G, et al. Neural correlates of consciousness in patients who have emerged from a minimally conscious state: a cross-sectional multimodal imaging study. Lancet Neurol. 2016;15: 830–42.

37. Hildebrandt IJ, Su H, Weber WA. Anesthesia and other considerations for in vivo imaging of small animals. ILAR J. 2008; 49:17–26.

38. Michenfelder JD, Milde JH. The relationship among canine brain temperature, metabolism, and function during hypothermia. Anesthesiology. 1991;75:130–6.

39. Lenz C, Frietsch T, Fütterer C, Rebel A, van Ackern K, Kuschinsky W, et al. Local coupling of cerebral blood flow to

cerebral glucose metabolism during inhalational anesthesia in rats: desflurane versus isoflurane. Anesthesiology. 1999;91: 1720–3.

40. Mielck F, Stephan H, Buhre W, Weyland A, Sonntag H. Effects of 1 MAC desflurane on cerebral metabolism, blood flow and carbon dioxide reactivity in humans. Br J Anaesth. 1998;81:155–60.

41. Frick T, Springe D, Grandgirard D, Leib SL, Haenggi M. An improved simple rat model for global cerebral ischaemia by induced cardiac arrest. Neurol Res. 2016;38:373–80.

42. Zuercher P, Springe D, Grandgirard D, Leib SL, Grossholz M, Jakob S, et al. A randomized trial of the effects of the noble gases helium and argon on neuroprotection in a rodent cardiac arrest model. BMC Neurol. 2016;16:43.

43. Dumas F, Bougouin W, Geri G, Lamhaut L, Bougle A, Daviaud F, et al. Is epinephrine during cardiac arrest associated with worse outcomes in resuscitated patients? J Am Coll Cardiol. 2014;64:2360–7.

44. Lehnert W, Gregoire M-C, Reilhac A, Meikle SR. Characterisation of partial volume effect and region-based correction in small animal positron emission tomography (PET) of the rat brain. Neuroimage. 2012;60:2144–57.

45. Rudolf J, Sobesky J, Ghaemi M, Heiss W-D. The correlation between cerebral glucose metabolism and benzodiazepine receptor density in the acute vegetative state. Eur J Neurol. 2002;9:671–7.

46. Hosmann A, Schober A, Gruber A, Sterz F, Testori C, Warenits A, et al. Cerebral and peripheral metabolism to predict successful reperfusion after cardiac arrest in rats: a microdialysis study. Neurocrit Care. 2016;24:283–93.

47. Reis C, Akyol O, Araujo C, Huang L, Enkhjargal B, Malaguit J, et al. Pathophysiology and the monitoring methods for cardiac arrest associated brain injury. Int J Mol Sci. 2017;18:129.

48. Drabek T, Foley LM, Janata A, Stezoski J, Kevin Hitchens T, Manole MD, et al. Global and regional differences in cerebral blood flow after asphyxial versus ventricular fibrillation cardiac arrest in rats using ASL-MRI. Resuscitation. 2014;85:964–71.